

Minimum Symbol Error Probability Low-Resolution Precoding for MU-MIMO Systems With PSK Modulation

Erico S. P. Lopes, *Graduate Student Member, IEEE*,

Lukas T. N. Landau, *Member, IEEE*, and Amine Mezghani, *Member, IEEE*

Abstract

We propose an optimal low-resolution precoding technique that minimizes the symbol error probability of the users. Unlike existing approaches that rely on QPSK modulation, for the derivation of the minimum symbol error probability objective function the current approach allows for any PSK modulation order. Moreover, the proposed method solves the corresponding discrete optimization problem optimally via a sophisticated branch-and-bound method. Moreover, we propose different approaches based on the greedy search method to compute practical solutions. Numerical simulations confirm the superiority of the proposed minimum symbol error probability criteria in terms of symbol error rate when compared with the established MMDDT and MMSE approaches.

Index Terms

Precoding, Constant Envelope, Low-Resolution Quantization, Phase Quantization, MIMO systems, Minimum Symbol Error Probability, Branch-and-Bound methods, Greedy Search Algorithms, Projection Based methods.

I. INTRODUCTION

Multuser multiple-input multiple-output (MU-MIMO) systems are considered as a promising physical-layer technique and are expected to be vital for future of wireless communications

E. S. P. Lopes and L. T. N. Landau are with the Centro de Estudos em Telecomunicações, Pontifícia Universidade Católica do Rio de Janeiro, Rio de Janeiro CEP 22453-900, Brazil, (e-mail: lukas.landau@cetuc.puc-rio.br; erico@cetuc.puc-rio.br). A. Mezghani is with the Department of Electrical and Computer Engineering, University of Manitoba, Winnipeg, MB, R3T 5V6, Canada, (e-mail: amine.mezghani@umanitoba.ca). This work has been supported by the ELIOT ANR18-CE40-0030 and FAPESP 2018/12579-7 project.

networks [1]. However, due to the high number of radio frequency front ends (RFFE) the energy consumption and hardware costs of the radio frequency chains impose a challenge for this kind of technology [2].

According to [3] energy efficiency (EE) will be a key feature of the next generation wireless communications networks. As stated in [4], 6G networks will require 10 to 100 times higher EE when compared to 5G, to enable scalable low-cost deployments, with low environmental impact, and better coverage. Another central demand for the future of wireless communications is higher data reliability, [5], [6]. As such, one challenge for MU-MIMO systems design is the increase in EE with minimum the bit-error-rate (BER) compromise.

To maximize the EE of MIMO systems, different studies, e.g. [7] and [8], have been conducted on how to decrease the energy consumption of a RFFE. One of the main approaches present in literature is to consider low-resolution data converters and constant envelope signaling. The main drawback of adopting these features is the performance degradation in the BER they yield.

A. Related Works

To mitigate the performance degradation low-resolution precoding have been receiving increasing attention of the wireless communications community. Several precoding strategies with low-resolution data converters exist in literature. Linear approaches, such as the phase Zero-Forcing (ZF-P) precoder [9], the Wiener Filter Quantized (WFQ) precoder [10] and the Sparse-ZF method [11], have been proposed and benefit from a relatively low computational complexity. However, to achieve a higher degree of reliability nonlinear symbol level precoding (SLP) methods have been presented based on different design criteria. The most popular criteria are the minimum mean squared error (MMSE) and the maximum minimum distance to the decision threshold (MMDDT).

For MMSE different SLP strategies have been presented. In [12] a 1-bit MMSE precoder was devised based on the semidefinite relaxation of the discrete feasible set. In [13] another MMSE based approach was proposed, this time employing a relaxation based on the infinity-norm for MU-MIMO-OFDM systems. In [14] a modified MMSE objective was considered and the feasible set was relaxed to its convex hull of a M-PSK modulation. In [15] a partial branch and bound (B&B) algorithm was considered in the context of QAM signaling for the 1-bit case. Using the MMSE criterion some optimal precoding approaches have also been developed. In [16] a sphere precoding strategy is utilized to compute the MMSE optimal transmit vector for

the 1-bit case. Moreover, the studies from [17] and [18] proposed different B&B techniques that yield the optimal MMSE precoding vector for any M-PSK modulation.

The MMDDT criterion, also called maximum safety margin (MSM) criterion or constructive interference (CI) criterion, have been receiving great attention of the community. In [19] different a constant envelope designs have been proposed based on the MMDDT criterion under per-antenna-power constraint. In [20] the MMDDT criterion is also utilized this time under the convex hull constraint. In [21] and [22] different greedy-search (GS) algorithms were developed using the MMDDT criterion for the 1-bit case with PSK modulation. The work from [22] is extended in [23] for QAM modulation. In [15] a partial B&B algorithm was considered in the context of PSK signaling for the 1-bit case. In [24] a B&B technique is utilized to compute the optimal MMDDT precoding vector also for the 1-bit case. Finally, the study from [25] generalizes the work from [24] for phase quantization with an arbitrary number of bits.

The study from [18] provides some useful insights about the relation between MMSE and MMDDT. Based on optimal transmit vectors [18] shown that the MMSE outperforms MMDDT in terms of BER for low-SNR regime, while the opposite is true for the high-SNR range. Different works, e.g. [25] and [26], claim that the MMDDT criterion performs optimally for the high-SNR regime in terms of symbol error rate (SER).

Aside from the MMSE and MMDDT criteria some works consider the direct optimization of symbol error probability (SEP) for precoding design e.g. [27]–[32]. While the studies from [27]–[30] mainly focus on QAM signaling with 1-bit data converters, [31] considers M-PSK modulation shows that by using the MMDDT design one can minimize an upper bound on the SEP. Another relevant result was achieved in [32] where an analytical formula for the SEP using QPSK data modulation is derived and, based on it, a discrete optimization problem is formulated.

B. Main Contributions

Following the direction from the works from [27]–[32] this study considers the direct minimization of the SEP (MSEP) criterion and focuses on the development of precoding techniques for a MU-MIMO downlink system with PSK modulation and phase quantization with an arbitrary number of bits.

In this context, we consider for the design objective the minimization of the exact SEP presented by [32] as the design criterion for the QPSK case and derive a novel MSEP formulation based on the union bound probability for higher-order PSK cases. Note that, the

proposed union-bound MSEP (UBMSEP) formulation, similarly as in the MMDDT case, relies on the minimization of an upper bound of the SEP. Numerical results confirm that the MSEP formulations outperform, in terms of SER, the MMSE criterion for medium and high SNR regime, while having similar performance for low-SNR, and outperform, in terms of SER, the MMDDT criterion for all examined SNR range.

The mentioned MSEP formulations are then utilized in conjunction with different optimization techniques to develop diverse precoding algorithms. First, projection based methods (PBMs) are considered as practical precoding techniques. PBM is a popular class of approaches present in literature, many works have utilized PBMs to devise practical precoding algorithms, e.g. [14], [18], [20]–[22], [33]. Then MSEP B&B approaches are considered for the computation of the optimal precoding vector. The proposed B&B algorithms differ from the ones present in literature, e.g. [17], [18], [24], [25], in terms of using a more restrictive pruning step which, then, contributes to a decreased average number of evaluated bounds and also in terms of the flexibility for choosing the projection step.

C. Remainder and Notation

The remainder of this paper is organized as follows: Section II describes the system model, whereas Section III exposes the derivation of the precoding design criteria. Section IV devises practical projection based precoding methods based on the presented formulations. Section V derives a B&B algorithm to compute the optimal MSEP solution. Section VI presents and discusses numerical results, while Section VII gives the conclusions. A convexity analysis is provided in the appendix.

Regarding the notation, bold lower case and upper case letters indicate vectors and matrices respectively. Non-bold letters express scalars. The operators $(\cdot)^*$ and $(\cdot)^T$ denote complex conjugation, transposition and Hermitian transposition, respectively. Real and imaginary part operator, as well as the functions $\Phi(\cdot)$, $Q(\cdot)$, $\text{erf}(\cdot)$ and $\log(\cdot)$, are also applied to vectors and matrices, e.g., $\text{Re}\{\mathbf{x}\} = [\text{Re}\{[\mathbf{x}]_1\}, \dots, \text{Re}\{[\mathbf{x}]_M\}]^T$.

II. SYSTEM MODEL

The system model, illustrated in Fig. 1, consists in a single-cell MU-MIMO scenario where the BS has perfect channel state information (CSI) and is equipped with M transmit antennas which serves K single antenna users.

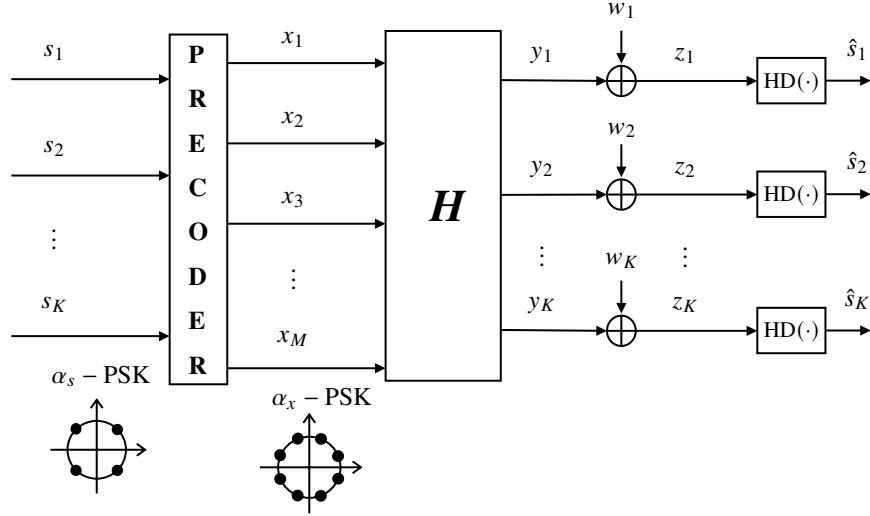


Fig. 1: Multiuser MIMO downlink with discrete precoding

In this study, a symbol level transmission is considered where s_k represents the data symbol to be delivered for the k -th user. Each symbol s_k is considered to belong to the set \mathcal{S} that represents all possible symbols of a α_s -PSK modulation and is given by

$$\mathcal{S} = \left\{ s : s = e^{\frac{j\pi(2i+1)}{\alpha_s}}, \text{ for } i = 1, \dots, \alpha_s \right\}. \quad (1)$$

The symbols of all users are described in a stacked vector notation as $\mathbf{s} = [s_1, \dots, s_K]^T \in \mathcal{S}^K$. It is considered that different users' symbols are independent meaning, $\mathbf{P}(s_i | s_j) = \mathbf{P}(s_i), \forall i \neq j$. Moreover it is assumed that all symbols have the same probability meaning $\mathbf{P}(s_k = s_i) = \frac{1}{\alpha_s}, \forall i \in 1, \dots, \alpha_s$. Based on \mathbf{s} the precoder computes the transmit vector $\mathbf{x} = [x_1, \dots, x_M]^T$, whose entries are constrained to the set \mathcal{X} , given by

$$\mathcal{X} = \left\{ x : x = e^{\frac{j\pi(2i+1)}{\alpha_x}}, \text{ for } i = 1, \dots, \alpha_x \right\}, \quad (2)$$

which describes an α_x -PSK alphabet. During this study the transmit vector \mathbf{x} will, many times, be described using real-valued notation as follows

$$\mathbf{x}_r = [\text{Re}\{\mathbf{x}_1\} \ \text{Im}\{\mathbf{x}_1\} \ \dots \ \text{Re}\{\mathbf{x}_M\} \ \text{Im}\{\mathbf{x}_M\}]^T. \quad (3)$$

The conversion operation from complex-valued to real-valued description is represented using the operator $R(\cdot)$. The opposite conversion, i.e. real-valued to complex-valued description, is denoted by the operator $C(\cdot)$.

The vector \mathbf{x} is transmitted over a frequency flat fading channel described by the matrix \mathbf{H} with coefficients $h_{k,m} = g_{k,m}\sqrt{\beta_k}$, where $g_{k,m}$ represents the complex small-scale fading between

the m -th antenna and the k -th user, and β_k denotes the real valued large-scale fading coefficient of the k -th user, $k = 1 \dots K$ and $m = 1 \dots M$. With this, the received signal corresponding to the k -th user is given by

$$\begin{aligned} z_k &= y_k + w_k \\ &= \mathbf{h}_k \mathbf{x} + w_k, \end{aligned} \quad (4)$$

where y_k is the noiseless received signal from the k -th user, \mathbf{h}_k is the k -th row of the channel matrix \mathbf{H} and the complex random variable $w_k \sim \mathcal{CN}(0, \sigma_w^2)$ represents additive white Gaussian noise (AWGN). Using stacked vector notation equation (4) can be extended to

$$\begin{aligned} \mathbf{z} &= \mathbf{y} + \mathbf{w} \\ &= \mathbf{H} \mathbf{x} + \mathbf{w}, \end{aligned} \quad (5)$$

where $\mathbf{z} = [z_1 \dots z_K]^T$, $\mathbf{y} = [y_1 \dots y_K]^T$ and $\mathbf{w} = [w_1 \dots w_K]^T$. Each received symbol z_k is, then, hard detected based on which decision region it belongs, meaning that z_k is detected as s_i if $z_k \in \mathcal{S}_i$. In the case of PSK modulation the decision regions are circle sectors with infinite radius and angle of 2θ , where θ is given by $\theta = \frac{\pi}{\alpha_s}$. As such the estimated symbol from the k -th user is given by $\hat{s}_k = \text{HD}(z_k)$, where $\text{HD}(\cdot)$ represents the hard detection operation. Finally, the estimated symbol vector can be written in stacked notation as $\hat{\mathbf{s}} = [\hat{s}_1, \dots, \hat{s}_K]$.

III. MSEP PRECODING FORMULATION

In this study we consider as the precoding design criterion the minimization of the SEP, or, equivalently, the maximization of the probability of correct detection. The probability of detecting the data vector \mathbf{s} conditioned on the transmit vector \mathbf{x} can be computed based on the probabilities of detection of the individual users as

$$\mathbb{P}(\hat{\mathbf{s}} = \mathbf{s} | \mathbf{x}) = \prod_{k=1}^K \mathbb{P}(\hat{s}_k = s_k | \mathbf{x}) . \quad (6)$$

To simplify the notation we denote $\mathbb{P}(\hat{\mathbf{s}} = \mathbf{s} | \mathbf{x})$ as $\mathbb{P}(\hat{\mathbf{s}} | \mathbf{x})$ and $\mathbb{P}(\hat{s}_k = s_k | \mathbf{x})$ as $\mathbb{P}(\hat{s}_k | \mathbf{x})$. With this, equation (6) is rewritten as

$$\mathbb{P}(\hat{\mathbf{s}} | \mathbf{x}) = \prod_{k=1}^K \mathbb{P}(\hat{s}_k | \mathbf{x}) . \quad (7)$$

As stated before, the detector decides for s_k when the received symbol z_k belongs to \mathcal{S}_k . Thus, the individual user probabilities are given by

$$P(\hat{s}_k|\mathbf{x}) = P(z_k \in \mathcal{S}_k|\mathbf{x}) = \frac{1}{\pi\sigma_w^2} \int \int_{\mathcal{S}_k} e^{-\frac{\|t-y_k\|_2^2}{\sigma_w^2}} dt. \quad (8)$$

The integral from (8), leads to two different formulations for the correct detection probability. The first corresponds to the specific case of QPSK the data modulation ($\alpha_s = 4$) and the second applies for any value of α_s .

A. QMSEP Problem Formulation

In this subsection, we expose the QPSK MSEP (QMSEP) formulation, which was first presented in [32]. When the data modulation is QPSK, $\text{Re}\{s_k\}$ and $\text{Im}\{s_k\}$ are independent and, thus, the decision regions \mathcal{S}_k can be written as $\mathcal{R}_k \cap \mathcal{I}_k$, where \mathcal{R}_k and \mathcal{I}_k are the decision regions the real and imaginary parts of s_k . The probability of the detector deciding for s_k is given by

$$\begin{aligned} P(\hat{s}_k|\mathbf{x}) &= P(z_k \in \mathcal{S}_k|\mathbf{x}) \\ P(\hat{s}_k|\mathbf{x}) &= P(\text{Re}\{z_k\} \in \mathcal{R}_k|\mathbf{x}) P(\text{Im}\{z_k\} \in \mathcal{I}_k|\mathbf{x}) \end{aligned} \quad (9)$$

With this, for $s_k = e^{j\frac{\pi}{4}}$,

$$\begin{aligned} P(z_k \in \mathcal{R}|\mathbf{x}) &= \int_0^\infty \frac{1}{\sqrt{\pi\sigma_w^2}} e^{-\frac{(t-\text{Re}\{\mathbf{h}_k\mathbf{x}\})^2}{\sigma_w^2}} dt = \Phi\left(\frac{\sqrt{2} \text{Re}\{\mathbf{h}_k\mathbf{x}\}}{\sigma_w}\right), \\ P(z_k \in \mathcal{I}|\mathbf{x}) &= \int_0^\infty \frac{1}{\sqrt{\pi\sigma_w^2}} e^{-\frac{(t-\text{Im}\{\mathbf{h}_k\mathbf{x}\})^2}{\sigma_w^2}} dt = \Phi\left(\frac{\sqrt{2} \text{Im}\{\mathbf{h}_k\mathbf{x}\}}{\sigma_w}\right). \end{aligned}$$

An expression for the correct decision probability can be achieved for all elements in \mathcal{S} as

$$P(\hat{s}_k|\mathbf{x}) = \Phi\left(\frac{\sqrt{2} \text{sign}(\text{Re}\{s_k\}) \text{Re}\{\mathbf{h}_k\mathbf{x}\}}{\sigma_w}\right) \Phi\left(\frac{\sqrt{2} \text{sign}(\text{Im}\{s_k\}) \text{Im}\{\mathbf{h}_k\mathbf{x}\}}{\sigma_w}\right). \quad (10)$$

With this, $P(s|\mathbf{x})$ is computed, for the QPSK case, by inserting (10) into (7), which reads as

$$P(\hat{s}|\mathbf{x}) = \prod_{k=1}^K \Phi\left(\frac{\sqrt{2} \text{sign}(\text{Re}\{s_k\}) \text{Re}\{\mathbf{h}_k\mathbf{x}\}}{\sigma_w}\right) \Phi\left(\frac{\sqrt{2} \text{sign}(\text{Im}\{s_k\}) \text{Im}\{\mathbf{h}_k\mathbf{x}\}}{\sigma_w}\right). \quad (11)$$

Based on (11) an optimization problem can be written for maximizing $P(s|\mathbf{x})$, which is cast as

$$\arg \max_{\mathbf{x} \in \mathcal{X}^M} \prod_{k=1}^K \Phi\left(\frac{\sqrt{2} \text{sign}(\text{Re}\{s_k\}) \text{Re}\{\mathbf{h}_k\mathbf{x}\}}{\sigma_w}\right) \Phi\left(\frac{\sqrt{2} \text{sign}(\text{Im}\{s_k\}) \text{Im}\{\mathbf{h}_k\mathbf{x}\}}{\sigma_w}\right). \quad (12)$$

Since the $\log(\cdot)$ is a monotonically increasing function, applying it to the objective from (12) does not change the optimal solution. The QPSK MSEP (QMSEP) optimization problem is, then, given by

$$\arg \min_{\mathbf{x} \in \mathcal{X}^M} - \sum_{k=1}^K \log \left(\Phi \left(\frac{\sqrt{2} \operatorname{sign}(\operatorname{Re}\{s_k\}) \operatorname{Re}\{\mathbf{h}_k \mathbf{x}\}}{\sigma_w} \right) \right) + \log \left(\Phi \left(\frac{\sqrt{2} \operatorname{sign}(\operatorname{Im}\{s_k\}) \operatorname{Im}\{\mathbf{h}_k \mathbf{x}\}}{\sigma_w} \right) \right). \quad (13)$$

An alternative real valued formulation of the QMSEP optimization problem can be cast as

$$\begin{aligned} \min_{\mathbf{x}_r} & - \sum_{k=1}^K \log(\Phi(\mathbf{h}_{R,k} \mathbf{x}_r)) + \log(\Phi(\mathbf{h}_{I,k} \mathbf{x}_r)) \\ \text{s.t.} & \quad x_{r,2m-1} + jx_{r,2m} \in \mathcal{X} \quad \text{for } m = 1, \dots, M. \end{aligned} \quad (14)$$

where $\mathbf{h}_{R,k}$ and $\mathbf{h}_{I,k}$ are the k -th rows of matrices \mathbf{H}_R and \mathbf{H}_I , respectively, which are defined as $\mathbf{H}_R = \frac{\sqrt{2}}{\sigma_w} \operatorname{diag}(\operatorname{sign}(\operatorname{Re}\{s\})) \mathbf{H}_R^Q$ and $\mathbf{H}_I = \frac{\sqrt{2}}{\sigma_w} \operatorname{diag}(\operatorname{sign}(\operatorname{Im}\{s\})) \mathbf{H}_I^Q$, with

$$\mathbf{H}_R^Q = \begin{bmatrix} \operatorname{Re}\{h_{11}\} & -\operatorname{Im}\{h_{11}\} & \cdots & \operatorname{Re}\{h_{1M}\} & -\operatorname{Im}\{h_{1M}\} \\ \vdots & \vdots & \ddots & \vdots & \vdots \\ \operatorname{Re}\{h_{K1}\} & -\operatorname{Im}\{h_{K1}\} & \cdots & \operatorname{Re}\{h_{KM}\} & -\operatorname{Im}\{h_{KM}\} \end{bmatrix}, \quad (15)$$

$$\mathbf{H}_I^Q = \begin{bmatrix} \operatorname{Im}\{h_{11}\} & \operatorname{Re}\{h_{11}\} & \cdots & \operatorname{Im}\{h_{1M}\} & \operatorname{Re}\{h_{1M}\} \\ \vdots & \vdots & \ddots & \vdots & \vdots \\ \operatorname{Im}\{h_{K1}\} & \operatorname{Re}\{h_{K1}\} & \cdots & \operatorname{Im}\{h_{KM}\} & \operatorname{Re}\{h_{KM}\} \end{bmatrix}. \quad (16)$$

The QMSEP formulation is limited for QPSK data modulation ($\alpha_s = 4$). In the following, we devise the MSEP formulation for higher order PSK modulations.

B. MSEP Problem formulation based on the Union Bound probability

When higher order PSK modulations are used, the decision regions cannot be written as the intersection of two independent regions. As such, the exact computation of the integral presented in (8) would lead to precoding algorithms with prohibitive computational complexity. Thus, for the MSEP formulation with $\alpha_s \neq 4$, we consider the maximization of a lower bound on the correct detection probability. The Union Bound, also known Boole's inequality [34], states that for any finite or countable set of events, the probability that at least one of the events happens is smaller or equal than the sum of the probabilities of the individual events, meaning

$$\mathbb{P} \left(\bigcup_i A_i \right) \leq \sum_i \mathbb{P}(A_i). \quad (17)$$

With this, the error probability for the k -th user, $P_e(\hat{s}_k|\mathbf{x})$, can be bounded by

$$\begin{aligned} P_e(\hat{s}_k|\mathbf{x}) &= P(z_k \in \mathcal{Z}_1 \cup \mathcal{Z}_2|\mathbf{x}) \\ &\leq P(z_k \in \mathcal{Z}_1|\mathbf{x}) + P(z_k \in \mathcal{Z}_2|\mathbf{x}), \end{aligned} \quad (18)$$

where the sets \mathcal{Z}_1 and \mathcal{Z}_2 are depicted in Fig. 2. When using the union bound, the error

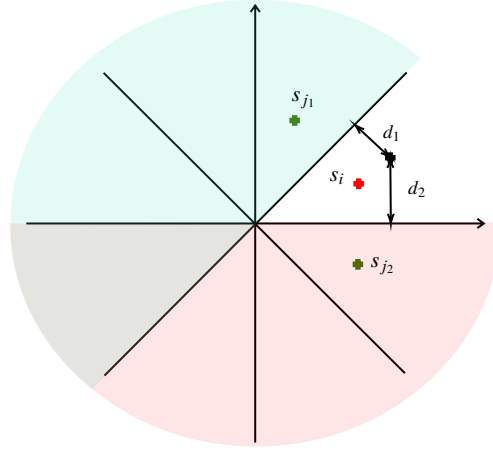


Fig. 2: Representation of the Union Bound

probability can be easily computed based on the minimum distances to the decision thresholds (MDDTs), $d_{1,k}$ and $d_{2,k}$, as

$$P(z_k \in \mathcal{Z}_1|\mathbf{x}) = \int_{d_{1,k}}^{\infty} \frac{1}{\sqrt{\pi\sigma_w^2}} e^{-\frac{t^2}{\sigma_w^2}} dt = Q\left(\frac{\sqrt{2} d_{1,k}}{\sigma_w}\right) \quad (19)$$

$$P(z_k \in \mathcal{Z}_2|\mathbf{x}) = \int_{d_{2,k}}^{\infty} \frac{1}{\sqrt{\pi\sigma_w^2}} e^{-\frac{t^2}{\sigma_w^2}} dt = Q\left(\frac{\sqrt{2} d_{2,k}}{\sigma_w}\right). \quad (20)$$

The MDDTs are computed, similarly to in [20] and [25], by applying a rotation of $\arg\{s_k^*\} = -\phi_{s_k}$ to the coordinate system such that the symbol of interest is placed on the real axis. This is done by multiplying both s_k and y_k by $e^{-j\phi_{s_k}}$ which results in

$$e^{-j\phi_{s_k}} s_k = 1, \quad \omega_k = e^{-j\phi_{s_k}} y_k. \quad (21)$$

Based on the rotated coordinate system the MDDTs are computed as

$$d_{1,k} = \text{Re}\{\omega_k\} \sin \theta - |\text{Im}\{\omega_k\}| \cos \theta \quad (22)$$

$$d_{2,k} = \text{Re}\{\omega_k\} \sin \theta + |\text{Im}\{\omega_k\}| \cos \theta, \quad (23)$$

which leads to an equivalent formulation as defining

$$d_{1,k} = \text{Re} \{s_k^* \mathbf{h}_k \mathbf{x}\} \sin \theta - \text{Im} \{s_k^* \mathbf{h}_k \mathbf{x}\} \cos \theta \quad (24)$$

$$d_{2,k} = \text{Re} \{s_k^* \mathbf{h}_k \mathbf{x}\} \sin \theta + \text{Im} \{s_k^* \mathbf{h}_k \mathbf{x}\} \cos \theta. \quad (25)$$

Based on the $d_{1,k}$ and $d_{2,k}$ one can construct a bound on the correct detection probability of the k -th user as

$$\begin{aligned} \mathbb{P}(\hat{s}_k | \mathbf{x}) &= 1 - \mathbb{P}_e(\hat{s}_k | \mathbf{x}) \\ &\geq 1 - (\mathbb{P}(z_k \in \mathcal{Z}_1 | \mathbf{x}) + \mathbb{P}(z_k \in \mathcal{Z}_2 | \mathbf{x})) \\ &= 1 - \mathbb{Q}\left(\frac{\sqrt{2} d_{1,k}}{\sigma_w}\right) - \mathbb{Q}\left(\frac{\sqrt{2} d_{2,k}}{\sigma_w}\right) \\ &= \frac{1}{2} \text{erf}\left(\frac{d_{1,k}}{\sigma_w}\right) + \frac{1}{2} \text{erf}\left(\frac{d_{2,k}}{\sigma_w}\right) \end{aligned} \quad (26)$$

With this, a bound for $\mathbb{P}(\mathbf{s} | \mathbf{x})$ is computed by inserting (26) into (7), which reads as

$$\mathbb{P}(\hat{\mathbf{s}} | \mathbf{x}) \geq \frac{1}{2^K} \prod_{k=1}^K \text{erf}\left(\frac{d_{1,k}}{\sigma_w}\right) + \text{erf}\left(\frac{d_{2,k}}{\sigma_w}\right). \quad (27)$$

Based on (27) an optimization problem can be cast as

$$\arg \max_{\mathbf{x} \in \mathcal{X}^M} \prod_{k=1}^K \text{erf}\left(\frac{d_{1,k}}{\sigma_w}\right) + \text{erf}\left(\frac{d_{2,k}}{\sigma_w}\right). \quad (28)$$

Since $\log(\cdot)$ is a monotonically increasing function, applying it to the objective from (28) yields an equivalent problem. With this, the union bound MSEP (UBMSEP) optimization problem for an α_s -PSK modulation, reads as

$$\arg \min_{\mathbf{x} \in \mathcal{X}^M} - \sum_{k=1}^K \log \left(\text{erf}\left(\frac{d_{1,k}}{\sigma_w}\right) + \text{erf}\left(\frac{d_{2,k}}{\sigma_w}\right) \right). \quad (29)$$

An alternative real valued formulation of the UBMSEP optimization problem can be cast as

$$\min_{\mathbf{x}_r} - \sum_{k=1}^K \log \left(\text{erf}\left(\left(\mathbf{h}_{R,\theta,k}^{s*} - \mathbf{h}_{I,\theta,k}^{s*}\right) \mathbf{x}_r\right) + \text{erf}\left(\left(\mathbf{h}_{R,\theta,k}^{s*} + \mathbf{h}_{I,\theta,k}^{s*}\right) \mathbf{x}_r\right) \right) \quad (30)$$

$$\text{s.t.} \quad x_{r,2m-1} + jx_{r,2m} \in \mathcal{X} \quad \text{for } m = 1, \dots, M.$$

where $\mathbf{h}_{R,\theta,k}^{s^*}$ and $\mathbf{h}_{I,\theta,k}^{s^*}$ are the k -th rows of matrices $\mathbf{H}_{R,\theta}^{s^*}$ and $\mathbf{H}_{I,\theta}^{s^*}$, respectively, which are defined as $\mathbf{H}_{R,\theta}^{s^*} = \frac{\sin(\theta)}{\sigma_w} \mathbf{H}_R^{s^*}$, and $\mathbf{H}_{I,\theta}^{s^*} = \frac{\cos(\theta)}{\sigma_w} \mathbf{H}_I^{s^*}$, with

$$\mathbf{H}_R^{s^*} = \begin{bmatrix} \operatorname{Re}\{h_{11}^{s^*}\} & -\operatorname{Im}\{h_{11}^{s^*}\} & \cdots & \operatorname{Re}\{h_{1M}^{s^*}\} & -\operatorname{Im}\{h_{1M}^{s^*}\} \\ \vdots & \vdots & \vdots & \vdots & \vdots \\ \operatorname{Re}\{h_{K1}^{s^*}\} & -\operatorname{Im}\{h_{K1}^{s^*}\} & \cdots & \operatorname{Re}\{h_{KM}^{s^*}\} & -\operatorname{Im}\{h_{KM}^{s^*}\} \end{bmatrix} \quad (31)$$

$$\mathbf{H}_I^{s^*} = \begin{bmatrix} \operatorname{Im}\{h_{11}^{s^*}\} & \operatorname{Re}\{h_{11}^{s^*}\} & \cdots & \operatorname{Im}\{h_{1M}^{s^*}\} & \operatorname{Re}\{h_{1M}^{s^*}\} \\ \vdots & \vdots & \vdots & \vdots & \vdots \\ \operatorname{Im}\{h_{K1}^{s^*}\} & \operatorname{Re}\{h_{K1}^{s^*}\} & \cdots & \operatorname{Re}\{h_{KM}^{s^*}\} & \operatorname{Im}\{h_{KM}^{s^*}\} \end{bmatrix}, \quad (32)$$

where $h_{ij}^{s^*}$ is the element of the i -th row and j -th column of the matrix $\mathbf{H}^{s^*} = \operatorname{diag}\{s^*\} \mathbf{H}$.

C. Considerations about the convexity of the MSEP formulations

Note that, the QMSEP objective function is convex, since $-\log(\Phi(\mathbf{A}\mathbf{x}))$ is convex in \mathbf{x} and the sum of convex function is also convex, c.f. [35]. As shown in appendix A the objective function of the UBMSEP formulation is convex for $(d_{1,k}, d_{2,k}) > (0, 0)$, $k \in 1, \dots, K$. To ensure a convex objective, the original UBMSEP problem is rewritten as

$$\begin{aligned} \min_{\mathbf{x}_r} & -\sum_{k=1}^K \log \left(\operatorname{erf} \left(\left(\mathbf{h}_{R,\theta,k}^{s^*} - \mathbf{h}_{I,\theta,k}^{s^*} \right) \mathbf{x}_r \right) + \operatorname{erf} \left(\left(\mathbf{h}_{R,\theta,k}^{s^*} + \mathbf{h}_{I,\theta,k}^{s^*} \right) \mathbf{x}_r \right) \right) \\ \text{s.t.} & \begin{bmatrix} \mathbf{H}_{R,\theta}^{s^*} - \mathbf{H}_{I,\theta}^{s^*} \\ \mathbf{H}_{R,\theta}^{s^*} + \mathbf{H}_{I,\theta}^{s^*} \end{bmatrix} \mathbf{x}_r \geq \mathbf{0}, \quad x_{r,2m-1} + jx_{r,2m} \in \mathcal{X} \quad \text{for } m = 1, \dots, M. \end{aligned} \quad (33)$$

Note that, the optimal solution from (29) is not necessarily the same as the optimal from (33). However, different solutions are only possible if, for at least one user, the optimal of (29) yields a noiseless received symbol y_i in the incorrect decision region. This leads to an optimal SEP, for this user, greater than half. This is, in general, not an interesting case, since future wireless communications systems will be designed to provide high reliability and, with this, avoid this kind of scenario.

Both MSEP optimization problems describe the minimization of a convex objective under a discrete feasible set. Note that, due to the discrete constraint $x_{r,2m} + jx_{r,2m+1} \in \mathcal{X}$ for $m = 1, \dots, M$ the MSEP problems are classified as a discrete programming problem (DPP). In the following sections optimal and suboptimal methods to solve the MSEP DPPs are proposed.

IV. MSEP PRECODING USING PROJECTION BASED METHODS

Projection based methods (PBMs) are prominent in literature due to its reduced computational complexity. Several works, e.g. [12], [17], [19], [20], [36]–[38], used PBMs with different design criteria. As such, in this section, different PBMs are considered to compute practical suboptimal solutions to (14) and (33).

PBMs rely on the relaxation of the non-convex feasible set to a larger convex set, such that, the optimization problem can be easily solved with standard optimization problem tools. The solution of the relaxed problem is, then, projected into the original feasible set which yields a suboptimal solution to the problem.

With this, we consider the relaxation of the discrete feasible set \mathcal{X}^M , to its convex hull \mathcal{P} . Note that the set \mathcal{P} is a polyhedron and, thus, can be described as the solution set of a finite number of linear equalities and inequalities [35]. Similarly as done in [17], [20] and [18] the relaxed feasible set is described in real-valued notation using the inequality $\mathbf{R} [\mathbf{x}_r^T, 1]^T \leq \mathbf{0}$, where $\mathbf{R} = \begin{bmatrix} \mathbf{A} & -\mathbf{b} \end{bmatrix}$ and

$$\mathbf{A} = \left[(\mathbf{I}_M \otimes \boldsymbol{\beta}_1)^T, (\mathbf{I}_M \otimes \boldsymbol{\beta}_2)^T, \dots, (\mathbf{I}_M \otimes \boldsymbol{\beta}_{\alpha_x})^T \right]^T, \quad (34)$$

$$\boldsymbol{\beta}_i = \begin{bmatrix} \cos \phi_i & -\sin \phi_i \end{bmatrix}, \quad \phi_i = \frac{2\pi i}{\alpha_x}, \text{ for } i = 1, \dots, \alpha_x, \quad \mathbf{b} = \frac{\cos(\frac{\pi}{\alpha_x})}{\sqrt{M}} \mathbf{1}_{M\alpha_x}. \quad (35)$$

In the remainder of this study the projection step is denoted by the operator $\mathcal{M}(\cdot)$. The details of the different methods for implementing $\mathcal{M}(\cdot)$ will be detailed in subsection IV-B. In what follows the relaxed optimization problems are formulated for each MSEP design criterion.

A. Relaxed Optimization Problems

As mentioned before, a PBM's first step is to relax \mathcal{X}^M to its convex hull \mathcal{P} . For the QMSEP case relaxing \mathcal{X}^M to \mathcal{P} leads to the following optimization problem

$$\begin{aligned} \min_{\mathbf{x}_r} & - \sum_{k=1}^K \log(\Phi(\mathbf{h}_{R,k} \mathbf{x}_r)) + \log(\Phi(\mathbf{h}_{I,k} \mathbf{x}_r)) \\ \text{s.t.} & \quad \mathbf{R} [\mathbf{x}_r^T, 1]^T \leq \mathbf{0}. \end{aligned} \quad (36)$$

Moreover, for the UBMSEP case the replacing \mathcal{X}^M by \mathcal{P} yields

$$\begin{aligned} \min_{\mathbf{x}_r} & - \sum_{k=1}^K \log \left(\operatorname{erf} \left(\left(\mathbf{h}_{R,\theta,k}^{s*} - \mathbf{h}_{I,\theta,k}^{s*} \right) \mathbf{x}_r \right) + \operatorname{erf} \left(\left(\mathbf{h}_{R,\theta,k}^{s*} + \mathbf{h}_{I,\theta,k}^{s*} \right) \mathbf{x}_r \right) \right) \\ \text{s.t.} & \begin{bmatrix} \mathbf{H}_{R,\theta}^{s*} - \mathbf{H}_{I,\theta}^{s*} \\ \mathbf{H}_{R,\theta}^{s*} + \mathbf{H}_{I,\theta}^{s*} \end{bmatrix} \mathbf{x}_r \geq \mathbf{0}, \quad \mathbf{R} [\mathbf{x}_r^T, 1]^T \leq \mathbf{0}. \end{aligned} \quad (37)$$

Note that, replacing \mathcal{X}^M by \mathcal{P} yields convex problems since both (36) and (37) minimize a convex objective under a convex feasible set.

B. Projection Methods

In the remainder of this work we denote the solution of the relaxed problems described in (36) and (37) as $\mathbf{x}_{r,\text{lb}}$ and its complex-valued description as \mathbf{x}_{lb} . Note that $\mathbf{x}_{\text{lb}} \in \mathcal{P}$ can also belong to the original feasible set \mathcal{X}^M as $\mathcal{P} \cap \mathcal{X}^M \neq \emptyset$. If this is the case \mathbf{x}_{lb} is also the optimal solution from the original problem and the projection step can be skipped. However, if $\mathbf{x}_{\text{lb}} \notin \mathcal{X}^M$ the precoding vector is computed as $\mathbf{x} = \mathcal{M}(\mathbf{x}_{\text{lb}})$. In what follows two different approaches for implementing $\mathcal{M}(\cdot)$ are exposed.

1) Projection Based on Uniform Quantization:

One of the most prominent projection methods present in literature is uniform quantization (UQ). When using this approach $\mathcal{M}(\cdot) = Q(\cdot)$, where $Q(\cdot)$ represents the quantization operation. The most common quantizing criterion is based on the elementwise Euclidean distance. As such, the p -th entry of the precoding vector \mathbf{x} , denoted as x^p , is computed as $x^p = \underset{i=1 \dots \alpha_x}{\operatorname{argmin}} |x_{\text{lb}}^p - x_i|^2$, where x_{lb}^p and x^p denotes the p -th entry of \mathbf{x}_{lb} and \mathbf{x} , respectively and x_i the i -th element of \mathcal{X} .

2) Projection via Greedy Search:

Although practical, UQ based projection can cause significant performance degradation. As such, in this subsection, this performance degradation is mitigated using GS as a local optimization approach. GS algorithms compute for each entry of the quantized vector \mathbf{x}_{ub} the value in \mathcal{X} which yield the smallest objective $g(\mathbf{x})$. When using the QMSEP criterion $g(\mathbf{x})$ is given by

$$g(\mathbf{x}) = -\mathbf{1}_K (\log(\Phi(\mathbf{S}_r \operatorname{Re}\{\mathbf{H}\mathbf{x}\})) + \log(\Phi(\mathbf{S}_i \operatorname{Im}\{\mathbf{H}\mathbf{x}\}))), \quad (38)$$

where $\mathbf{S}_r = \frac{\sqrt{2}}{\sigma_w} \operatorname{diag}(\operatorname{sign}(\operatorname{Re}\{\mathbf{s}\}))$ and $\mathbf{S}_i = \frac{\sqrt{2}}{\sigma_w} \operatorname{diag}(\operatorname{sign}(\operatorname{Im}\{\mathbf{s}\}))$. For the UBMSEP case $g(\mathbf{x})$ reads as

$$g(\mathbf{x}) = -\mathbf{1}_K \log(\operatorname{erf}(\operatorname{Re}\{\mathbf{H}^s \mathbf{x}\} - \operatorname{Im}\{\mathbf{H}^c \mathbf{x}\}) + \operatorname{erf}(\operatorname{Re}\{\mathbf{H}^s \mathbf{x}\} + \operatorname{Im}\{\mathbf{H}^c \mathbf{x}\})), \quad (39)$$

where $\mathbf{H}^s = \frac{\sin(\theta)}{\sigma_w} \text{diag}(\mathbf{s}^*) \mathbf{H}$ and $\mathbf{H}^c = \frac{\cos(\theta)}{\sigma_w} \text{diag}(\mathbf{s}^*) \mathbf{H}$. In this subsection two GS methods are considered for implementing $\mathcal{M}(\cdot)$. The first is a partial GS approach where only the entries of \mathbf{x}_{lb} which do not belong to \mathcal{X} are evaluated. The second is a full GS method where all entries of \mathbf{x}_{lb} are considered. In the following, the steps of the methods are detailed. Algorithm 1 exposes the partial GS approach while Algorithm 2 details the full GS method. Regarding notation P denotes the length of the input vector.

Algorithm 1 Partial-GS Projection Algorithm

Inputs: $\mathbf{x}_{\text{ub}}, \mathbf{x}_{\text{lb}}$ and $g(\mathbf{x})$ **Output:** \mathbf{x}_{out}

Construct the set $\mathcal{T} = \{p : x_{\text{lb}}^p \notin \mathcal{X}\}$

for $p \in \mathcal{T}$ **do**

for $i = 1 : \alpha_x$ **do**

 Fix x_{ub}^p as x_i and compute the $g_p^i = g(\mathbf{x}_{\text{ub}})$

end for

 Update the p -th entry of \mathbf{x}_{ub} as $x_{\text{ub}}^p = \arg \min_{i=1, \dots, \alpha_x} g_p^i$

end for

The output vector is given by $\mathbf{x}_{\text{out}} = \mathbf{x}_{\text{ub}}$

Algorithm 2 Full-GS Projection Algorithm

Inputs: $\mathbf{x}_{\text{ub}}, g(\mathbf{x})$ and P **Output:** \mathbf{x}_{out}

for $p = 1 : P$ **do**

for $i = 1 : \alpha_x$ **do**

 Fix x_{ub}^p as x_i and compute the $g_p^i = g(\mathbf{x}_{\text{ub}})$

end for

 Update the p -th entry of \mathbf{x}_{ub} as $x_{\text{ub}}^p = \arg \min_{i=1, \dots, \alpha_x} g_p^i$

end for

The output vector is given by $\mathbf{x}_{\text{out}} = \mathbf{x}_{\text{ub}}$

V. OPTIMAL MSEP PRECODING VIA BRANCH-AND-BOUND

In this section, we devise algorithms that solve optimally the DPPs described in (14) and (33). According to [39], the most established class of approaches for solving a DPP with reasonable computational complexity is the B&B. First created in 1960 by A. H. Land and A. G. Doig [40] the essence of B&B methods consists in eliminating, as many as possible, candidate solutions,

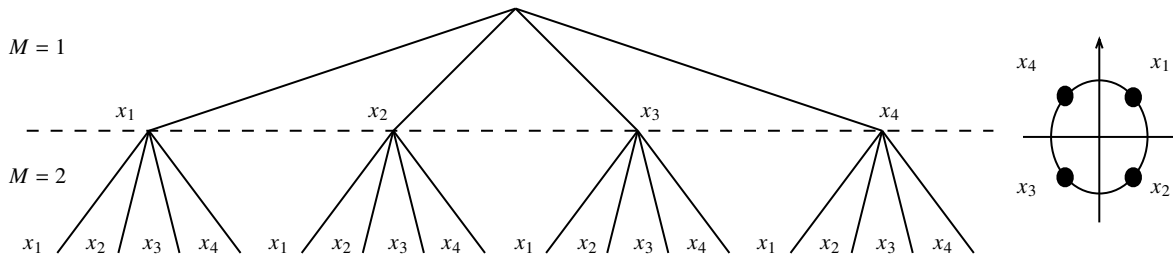


Fig. 3: Tree representation of the set \mathcal{X}^M for a system with $M = 2$ BS antennas and QPSK precoding modulation ($\alpha_x = 4$)

such that, the optimal can be computed using exhaustive search. The basics of precoding using B&B method can be found well detailed in the works from [17], [18], [24], [25], as such, this study will focus on the specifics of the proposed B&B algorithms.

A. Branch-and-Bound as a Tree Search Method

A B&B algorithm is a tree search based method where the tree represents the feasible set. For the case of the problems defined in (14) and (33) the feasible set of the optimization variable is \mathcal{X}^M . As such, in this subsection we show how \mathcal{X}^M is represented in the form of a tree.

For the construction of the tree it is considered that the p -th BS antenna represents the p -th layer and each possibility for a subvector $\mathbf{f} \in \mathcal{X}^p$ represents one branch. With this, the tree has M layers with α_x^M branches in the last layer. An example of a tree representation of the feasible set is shown in Fig. 3 for the case of two transmit antennas at the BS and QPSK signaling.

B. Subproblem formulation

In a B&B algorithm a DPP is solved by considering partially fixed subvectors and computing upper and lower bounds to evaluate if the fixed subvector is part of the optimal solution. In this subsection, we describe, for each different MSEP formulation, the optimization problems that are solved in each layer of the B&B algorithm to compute the lower bounding step.

As mentioned in subsection V-A, the branches of the tree represent a subvector $\mathbf{f} \in \mathcal{X}^p$ for the p -th layer. With this, the subproblems are derived by fixing, for each branch, the corresponding subvector \mathbf{f} and optimizing the remaining subvector $\mathbf{v} \in \mathcal{X}^{M-p}$, as such the transmit vector is given by $\mathbf{x} = [\mathbf{f}^T, \mathbf{v}^T]^T$. However, such that the optimization problems are real-valued, in this study it is considered the division of \mathbf{x}_r instead of \mathbf{x} , which reads as

$$\mathbf{x}_r = \left[\mathbf{f}_r^T, \mathbf{v}_r^T \right]^T, \quad (40)$$

where for the p -th layer, the length of the fixed subvector \mathbf{f}_r is $2p$ and, consequently, the length of the subvector \mathbf{v}_r is $2(M - p)$. The subproblems are then derived based on the formulation of the relaxed PBM problems from subsection IV-A.

1) *QMSEP Subproblem formulation:*

The QMSEP subproblems are written considering the minimization of the objective function shown in (38) for a given \mathbf{f}_r . To this end, the matrices \mathbf{H}_R and \mathbf{H}_I are divided as

$$\mathbf{H}_R = \begin{bmatrix} \mathbf{F}_R & \mathbf{V}_R \end{bmatrix} \quad \mathbf{H}_I = \begin{bmatrix} \mathbf{F}_I & \mathbf{V}_I \end{bmatrix} \quad (41)$$

where \mathbf{F}_R and \mathbf{F}_I consist of the first $2p$ columns of \mathbf{H}_R and \mathbf{H}_I , respectively and \mathbf{V}_R and \mathbf{V}_I consist of the subsequent $2(M - p)$ columns of \mathbf{H}_R and \mathbf{H}_I , respectively. With this, the subproblem conditioned on \mathbf{f}_r reads as

$$\begin{aligned} \min_{\mathbf{v}_r} & -\mathbf{1}_K (\log(\Phi(\mathbf{F}_R \mathbf{f}_r + \mathbf{V}_R \mathbf{v}_r)) + \log(\Phi(\mathbf{F}_I \mathbf{f}_r + \mathbf{V}_I \mathbf{v}_r))) \\ \text{s.t.} & \quad \mathbf{R}' [\mathbf{v}_r^T, 1]^T \leq \mathbf{0}, \end{aligned} \quad (42)$$

where $\mathbf{R}' = [\mathbf{A}', -\mathbf{b}']$ is obtained by selecting the last $2(M - p)$ columns of \mathbf{R} .

2) *UBMSEP Subproblem formulation:*

Similarly as in the QMSEP case, the matrices \mathbf{H}_R^{s*} and \mathbf{H}_I^{s*} are divided as

$$\mathbf{H}_R^{s*} = \begin{bmatrix} \mathbf{F}_{R,\theta}^{s*} & \mathbf{V}_{R,\theta}^{s*} \end{bmatrix} \quad \mathbf{H}_I^{s*} = \begin{bmatrix} \mathbf{F}_{I,\theta}^{s*} & \mathbf{V}_{I,\theta}^{s*} \end{bmatrix}. \quad (43)$$

As such, the subproblem associated with the fixed vector \mathbf{f}_r is given by

$$\begin{aligned} \min_{\mathbf{v}_r} & -\mathbf{1}_K \left(\log \left(\text{erf} \left(\mathbf{F}_{R,\theta}^{s*} \mathbf{f}_r + \mathbf{V}_{R,\theta}^{s*} \mathbf{v}_r - \mathbf{F}_{I,\theta}^{s*} \mathbf{f}_r + \mathbf{V}_{I,\theta}^{s*} \mathbf{v}_r \right) + \text{erf} \left(\mathbf{F}_{R,\theta}^{s*} \mathbf{f}_r + \mathbf{V}_{R,\theta}^{s*} \mathbf{v}_r + \mathbf{F}_{I,\theta}^{s*} \mathbf{f}_r + \mathbf{V}_{I,\theta}^{s*} \mathbf{v}_r \right) \right) \right) \\ \text{s.t.} & \quad \begin{bmatrix} \mathbf{V}_{R,\theta}^{s*} - \mathbf{V}_{I,\theta}^{s*} \\ \mathbf{V}_{R,\theta}^{s*} + \mathbf{V}_{I,\theta}^{s*} \end{bmatrix} \mathbf{v}_r \geq - \begin{bmatrix} \mathbf{F}_{R,\theta}^{s*} - \mathbf{F}_{I,\theta}^{s*} \\ \mathbf{F}_{R,\theta}^{s*} + \mathbf{F}_{I,\theta}^{s*} \end{bmatrix} \mathbf{f}_r, \quad \mathbf{R}' [\mathbf{v}_r^T, 1]^T \leq \mathbf{0}. \end{aligned} \quad (44)$$

C. Proposed MSEP Branch-and-Bound Algorithms

In this subsection a B&B algorithm is assembled with the tools previously presented. Utilizing the B&B algorithm requires choosing a MSEP criterion and a projection method. As such, it is considered $\mathcal{M}(\cdot)$, the criterion utilized and consequently $g(\mathbf{x})$ as inputs of the algorithm.

1) Initialization Step:

In the proposed MSEP B&B algorithms an initialization step is considered. As such, the relaxed problem, described in subsection IV-A, corresponding to the chosen criterion is solved which yields $\mathbf{x}_{r,lb}$. Subsequently, the projection step is performed which yields $\check{\mathbf{x}} = \mathcal{M}(C(\mathbf{x}_{r,lb}))$. Note that, as mentioned in [17] and [18], if $\mathbf{x}_{lb} = \check{\mathbf{x}}$ the algorithm returns $\check{\mathbf{x}}$ as it is the optimal solution. Otherwise, $\check{g} = g(\check{\mathbf{x}})$ is computed as the initial smallest known upper bound and both \check{g} and $\check{\mathbf{x}}$ are stored.

2) Tree search process:

For the tree search process breadth first search is considered. The process starts by setting the layer value $p = 1$ and, accordingly, solving the subproblems which yields the solution $\mathbf{v}_{r,lb|f}$. The vector $\mathbf{x}_{lb|f} = \left[\mathbf{f}^T, C(\mathbf{v}_{r,lb|f})^T \right]^T$ is, then, constructed and the value of $g(\mathbf{x}_{lb|f})$ is computed and stored. The solution subvector $\mathbf{v}_{lb|f}$ is projected to \mathcal{X}^{M-p} which yields $\mathbf{v}_{ub|f} = \mathcal{M}(\mathbf{v}_{lb|f})$. With this, one can construct $\mathbf{x}_{ub|f} = \left[\mathbf{f}^T, \mathbf{v}_{ub|f}^T \right]^T$. Note that, $\mathbf{x}_{ub|f} \in \mathcal{X}^M$ is an upper bound solution, and thus, $g(\mathbf{x}_{ub|f})$ is an upper bound on $g(\mathbf{x}_{opt})$, with \mathbf{x}_{opt} being the optimal solution.

To evaluate if $g(\mathbf{x}_{ub|f})$ is the smallest known upper bound the condition $g(\mathbf{x}_{ub|f}) < \check{g}$ is checked. If true, the smallest known upper bound and its corresponding value of \mathbf{x} are updated as $\check{g} = g(\mathbf{x}_{ub|f})$ and $\check{\mathbf{x}} = \mathbf{x}_{ub|f}$.

After all possible valid branches in one layer are evaluated, i.e. all valid values of \mathbf{f} were fixed and its conditioned upper and lower bounds computed, they are considered in the pruning process. The pruning step is explained in details in the following subsection. After pruning, the set of valid \mathbf{f} subvectors is updated and the algorithm repeats this process in the next layer. In the last layer, it is expected that only a few valid candidate solutions remain. As such, they are all evaluated against $\check{\mathbf{x}}$ and the optimal value is determined by the vector that yields the minimum value of the objective function. Note that the optimal solution might not be in the last layer as it could be found in previous layers.

3) Pruning Step:

To determine if a fixed subvector \mathbf{f} is valid, i.e. if it can be a subvector of the optimal solution \mathbf{x}_{opt} , the stored values $g(\mathbf{x}_{lb|f})$ are compared with \check{g} . In this work, a subvector is considered as valid if $g(\mathbf{x}_{lb|f}) < (1 - \gamma)\check{g}$, where $0 < \gamma \leq 1$, which yields a solution in the ϵ -suboptimal set.

When evaluating the p -th layer for a branch, which is the same as evaluating the p -th layer for a subvector \mathbf{f} , it holds that $g(\mathbf{x}_{lb|f}) \leq g(\mathbf{x}_{ub|f})$. Consider now the scenario where $\mathbf{x}_{ub|f} = \mathbf{x}_{opt}$ and $g(\mathbf{x}_{opt}) = g(\mathbf{x}_{lb|f})$. In this case, using the mentioned pruning condition, the optimal branch

is considered as not valid if $g(\mathbf{x}_{\text{opt}}) \geq (1 - \gamma)\check{g}$. This results in the algorithm returning $\check{\mathbf{x}}$ when $g(\mathbf{x}_{\text{opt}}) \leq \check{g} \leq \frac{g(\mathbf{x}_{\text{opt}})}{1-\gamma}$. This means that the algorithm allows for any solution in the ϵ -suboptimal set given by $\mathcal{X}_{\text{opt},\epsilon} = \{\mathbf{x} : g(\mathbf{x}) \leq g(\mathbf{x}_{\text{opt}}) + \epsilon\}$, cf. [35], where $\epsilon = g(\mathbf{x}_{\text{opt}})\frac{\gamma}{1-\gamma}$.

Allowing for a transmit vector in the ϵ -suboptimal theoretically could yield a suboptimal solution. However, due to the discrete nature of the feasible set, one can choose a sufficiently small value for γ , for example $\gamma = \delta\check{g}$ which yields $\epsilon = g(\mathbf{x}_{\text{opt}})\frac{\delta\check{g}}{1-\delta\check{g}}$ with $0 \leq \delta \ll 1$, such that $\mathcal{X}_{\text{opt},\epsilon}$ contains only the global optimal solution \mathbf{x}_{opt} .

By setting a sufficiently small value for δ , the output solution of the proposed B&B algorithm corresponds, with probability one, to the optimal solution \mathbf{x}_{opt} of the corresponding MSEP problem, as is confirmed by the numerical results shown in Section VI. The steps of the MSEP B&B algorithm are detailed in Algorithm 3.

Algorithm 3 Proposed MSEP B&B Precoding Algorithm

Inputs: $\mathcal{M}(\cdot)$, $g(\mathbf{x})$ and MSEP criterion **Output:** \mathbf{x}_{out}

Solve the relaxed optimization problem corresponding to the MSEP criterion and get $\mathbf{x}_{\text{r,lb}}$

Project $\mathbf{x}_{\text{lb}} = R(\mathbf{x}_{\text{r,lb}})$ to get the upper bound solution $\mathbf{x}_{\text{ub}} = \mathcal{M}(\mathbf{x}_{\text{lb}})$

If $\mathbf{x}_{\text{ub}} == \mathbf{x}_{\text{lb}}$

return $\mathbf{x}_{\text{out}} = \mathbf{x}_{\text{ub}}$

end if

Define $\check{\mathbf{x}} = \mathbf{x}_{\text{ub}}$ and compute $\check{g} = g(\check{\mathbf{x}})$

Define the first level ($p = 1$) of the tree by $\mathcal{G}_p := \mathcal{X}$

for $p = 1 : M - 1$ **do**

 Partition \mathcal{G}_p in $f_1, \dots, f_{|\mathcal{G}_p|}$

for $i = 1 : |\mathcal{G}_p|$ **do**

 Conditioned on $f_{\text{r},i} = R(f_i)$ solve the subproblem corresponding to the MSEP criterion to get $\mathbf{v}_{\text{r,lb}|f_i}$

 Construct $\mathbf{x}_{\text{lb},i} = \left[f_i^T, C(\mathbf{v}_{\text{r,lb}|f_i})^T \right]$ and determine the lower bound $g_{\text{lb},i} = g(\mathbf{x}_{\text{lb},i})$

 Compute the upper bound $\mathbf{x}_{\text{ub},i} = \mathcal{M}(\mathbf{x}_{\text{lb},i})$

 With $\mathbf{x}_{\text{ub},i}$ compute the upper bound $g_{\text{ub},i} = g(\mathbf{x}_{\text{ub},i})$

 Update the best upper bound as $\check{g} = \min(\check{g}, g_{\text{ub},i})$ and update $\check{\mathbf{x}}$ accordingly

end for

 Construct a reduced set by comparing conditioned lower bounds with the global upper bound \check{g}

$\mathcal{G}'_p := \{\mathbf{x}_{\text{lb},i} \mid g_{\text{lb},i} < (1 - \gamma)\check{g}, i = 1, \dots, |\mathcal{G}_p|\}$

 Define the set for the next level in the tree: $\mathcal{G}_{p+1} := \mathcal{G}'_p \times \mathcal{X}$

end for

The global solution is $\mathbf{x}_{\text{out}} = \underset{\mathbf{x} \in \{\mathcal{G}_M \cup \{\check{\mathbf{x}}\}\}}{\text{argmin}} g(\mathbf{x})$

VI. NUMERICAL RESULTS

For the numerical evaluation, the SER is considered. We assume that the channel gains are modeled by independent Rayleigh fading [41], meaning $\beta_m = 1$ for $m = 1, \dots, M$ and $g_{k,m} \sim \mathcal{CN}(0, \sigma_g^2)$ for $k = 1, \dots, K$ and $m = 1, \dots, M$ as done implicitly in [9] and [20] and explicitly in [19]. Moreover, the SNR is defined by $\text{SNR} = \frac{\|\mathbf{x}\|_2^2}{N_0}$, where the spectral noise power density N_0 is equivalent to the noise sample variance σ_w^2 . For the MSEP B&B methods δ is set to $\delta = 5 \cdot 10^{-7}$.

This section is divided in three parts. In the first, the proposed MSEP formulations are evaluated against other state-of-the-art criteria. In the second, the proposed methods are compared with other state-of-the-art algorithms in terms of SER. Finally, in the third, a complexity analysis is performed and the proposed approaches are compared with the state-of-the-art techniques both in terms of runtime.

The state-of-the-art methods considered for comparison in this study are

1. The MSM-Precoder [20] considering phase quantization;
2. The ZF precoder with constant envelope [9], where the entries of the precoding vector are subsequently phase quantized;
3. The phase quantized CIO precoder implemented via CVX [19];
4. The single-carrier version of the SQUID-OFDM precoder [13] phase quantized;
6. The C3PO precoder [42] phase quantized considering a real valued scaling factor;
7. The MMDDT branch-and-bound precoder [25];
8. The MMSE branch-and-bound precoder [17];

A. Criteria comparison

For the criteria comparison we consider two different scenarios. In the first, both MSEP criteria are compared with the MMSE and MMDDT criteria using QPSK data symbols. In the second, only the UBMSEP criterion is compared with the MMSE and MMDDT criterion using 8-PSK data symbols.

As can be seen in Fig. 4, the QMSEP criterion outperforms all other state-of-the-art criteria for most of the SNR range, having the same performance as MMSE for low-SNR regime. The UBMSEP method presents does not present significant decrease in performance when compared with the QMSEP approach. As shown in Fig. 5, the UBMSEP criterion also outperforms in terms of SER the state-of-the-art design criteria when using higher order PSK modulations. As

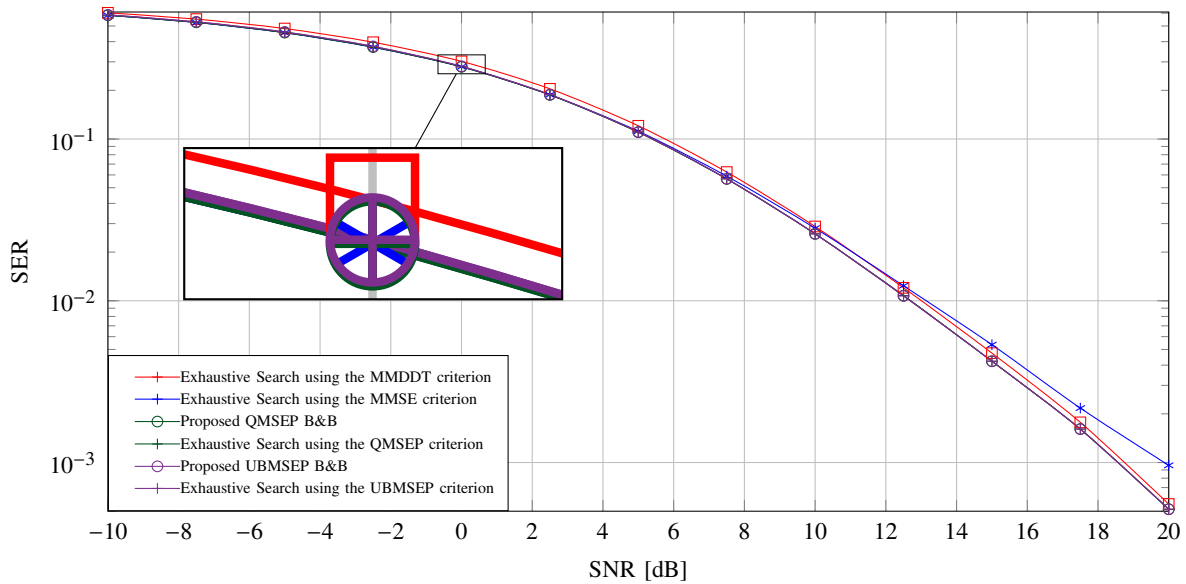


Fig. 4: SER versus SNR for $K = 2$, $M = 5$, $\alpha_s = 4$ and $\alpha_x = 4$

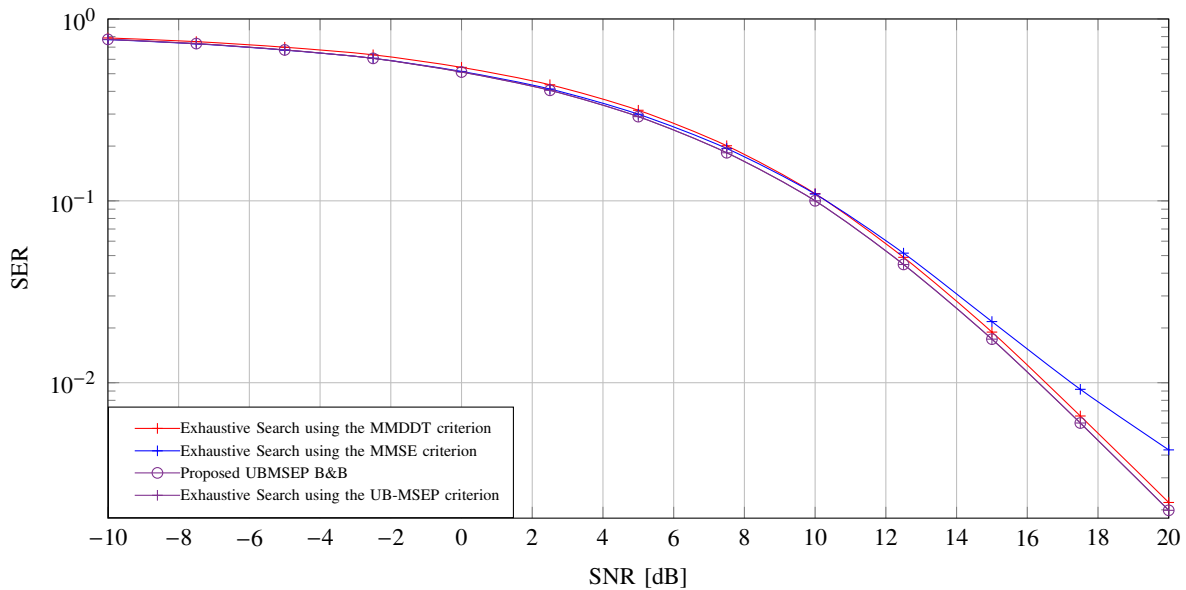


Fig. 5: SER versus SNR for $K = 2$, $M = 5$, $\alpha_s = 8$ and $\alpha_x = 8$

expected UBMSEP outperforms MDDT criterion for all examined SNR range and outperforms the MMSE criterion for medium and high-SNR regime. Finally, as expected the MSEP B&B algorithm yields the same result as exhaustive search for both MSEP criteria.

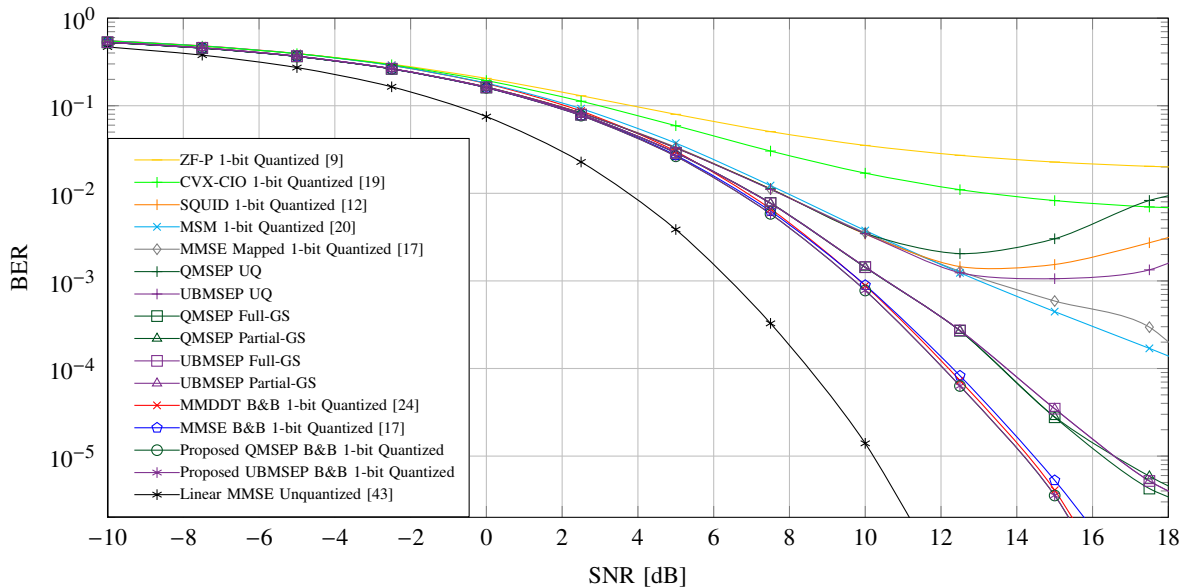


Fig. 6: SER versus SNR for $K = 3$, $M = 12$, $\alpha_s = 4$ and $\alpha_x = 4$

B. SER comparison with the state-of-the-art

In this subsection the proposed methods are compared, in terms of SER, against the mentioned state-of-the-art techniques considering the scenario of $K = 3$ users, $M = 12$ BS antennas, QPSK data symbols and QPSK transmit symbols.

As shown in Fig. 6, the proposed B&B methods outperform all other state-of-the-art approaches in terms of SER. Note that this was expected since the proposed methods compute the optimal transmit vector using as the criterion the minimization of the SEP. Moreover, as can be seen in Fig. 6 using the MSEP criteria in conjunction with PBMs based on UQ yield SER degradation for high-SNR. In this context, both Full-GS and Partial-GS algorithms mitigate the performance loss due to projection and outperform all other investigated state-of-the-art approaches.

C. Complexity Analysis

In this section, the complexity of the proposed methods is evaluated against the mentioned state-of-the-art approaches considering the same scenario utilized in the previous subsection, $K = 3$ users $M = 12$ BS antennas and QPSK data and transmit vector symbols. The complexity of the proposed B&B approaches is measured using the different methods for projection presented

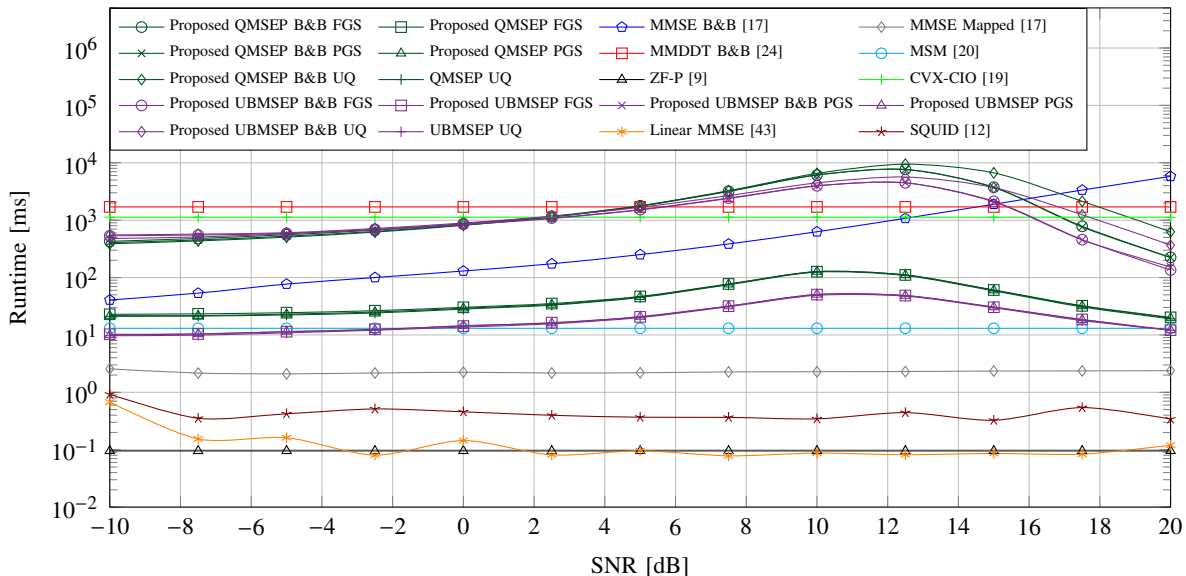


Fig. 7: Runtime (ms) versus SNR, $K = 3$, $M = 12$, $\alpha_s = 4$ and $\alpha_x = 4$

in section IV. As mentioned before, the proposed methods are evaluated against the state-of-the-art approaches in terms of the runtime. For solving the optimization problems for the methods in [17], [20], [25] and for the proposed approaches the optimization toolbox from Matlab was utilized. The optimization problem required for the CVX-CIO approach [19] was solved via CVX [35], as suggested by the authors. The results are shown in Fig. 7.

As can be seen in Fig. 7 the proposed MSEP-GS methods have similar runtime when compared with the MSEP projection methods using UQ. Moreover, the proposed MSEP-GS approaches have significantly smaller runtime when compared with the optimal B&B techniques which confirms the suitability of the proposed MSEP-GS methods as reasonable complexity performance tradeoff approaches. As also shown in Fig. 7 the proposed B&B methods have smaller runtime than the MMDDT B&B approach from [24] for most of the SNR range analyzed and also outperforms the MMSE B&B approach from [17] for high SNR.

VII. CONCLUSIONS

In this study we propose a novel precoding criterion based on the direct minimization of the SEP for quantized signals with constant envelope and PSK modulation. Unlike the existing MSEP designs [27]–[32] the proposed approaches allow for any PSK modulation order and phase quantization with any number of bits. Using the proposed criterion and the one from [32]

this study develops optimal precoding techniques based on a sophisticated B&B algorithm and practical precoding methods based on GS.

Numerical results show that the proposed optimal approaches outperforms the existing methods, in terms of SER for all investigated SNR range. Numerical results also indicate that the proposed optimal methods have less computational complexity for some scenarios when compared with other B&B approaches. The proposed GS algorithms also outperform all other state-of-the-art suboptimal methods in terms of SER with decreased complexity when compared with the optimal approaches. As such, reasonable complexity performance tradeoffs can be achieved using the proposed GS techniques.

APPENDIX

A. Convexity analysis of the UBMSEP objective

This appendix derives the conditions for convexity of the UBMSEP objective function. In this analysis it is considered the real-valued UBMSEP formulation described in (30). With this, the UBSMEP objective can be cast as

$$g(\mathbf{x}_r) = - \sum_{k=1}^K \log \left(\operatorname{erf} \left(\left(\mathbf{h}_{R,\theta,k}^{s*} - \mathbf{h}_{I,\theta,k}^{s*} \right) \mathbf{x}_r \right) + \operatorname{erf} \left(\left(\mathbf{h}_{R,\theta,k}^{s*} + \mathbf{h}_{I,\theta,k}^{s*} \right) \mathbf{x}_r \right) \right). \quad (45)$$

To simplify the notation the vectors $\mathbf{h}_{1,k}$ and $\mathbf{h}_{2,k}$ are introduced as $\mathbf{h}_{1,k} = \mathbf{h}_{R,\theta,k}^{s*} - \mathbf{h}_{I,\theta,k}^{s*}$ and $\mathbf{h}_{2,k} = \mathbf{h}_{R,\theta,k}^{s*} + \mathbf{h}_{I,\theta,k}^{s*}$. With this, $g(\mathbf{x}_r)$ is rewritten as

$$g(\mathbf{x}_r) = - \sum_{k=1}^K \log \left(\operatorname{erf} (\mathbf{h}_{1,k} \mathbf{x}_r) + \operatorname{erf} (\mathbf{h}_{2,k} \mathbf{x}_r) \right) \quad (46)$$

Convexity can be proven by evaluating the conditions in which the Hessian is positive semi-definite (PSD). To this end the in what follows the Hessian is calculated. Taking the derivative of $g(\mathbf{x}_r)$ with respect to \mathbf{x}_r

$$\frac{\partial g(\mathbf{x}_r)}{\partial \mathbf{x}_r} = - \sum_{k=1}^K \frac{\partial}{\partial \mathbf{x}_r} \log \left(\operatorname{erf} (\mathbf{h}_{1,k} \mathbf{x}_r) + \operatorname{erf} (\mathbf{h}_{2,k} \mathbf{x}_r) \right) \quad (47)$$

$$= - \sum_{k=1}^K \frac{\frac{\partial}{\partial \mathbf{x}_r} \left(\operatorname{erf} (\mathbf{h}_{1,k} \mathbf{x}_r) + \operatorname{erf} (\mathbf{h}_{2,k} \mathbf{x}_r) \right)}{\operatorname{erf} (\mathbf{h}_{1,k} \mathbf{x}_r) + \operatorname{erf} (\mathbf{h}_{2,k} \mathbf{x}_r)} \quad (48)$$

$$= - \sum_{k=1}^K \frac{\frac{2}{\sqrt{\pi}} e^{-(\mathbf{h}_{1,k} \mathbf{x}_r)^2} \mathbf{h}_{1,k} + \frac{2}{\sqrt{\pi}} e^{-(\mathbf{h}_{2,k} \mathbf{x}_r)^2} \mathbf{h}_{2,k}}{\operatorname{erf} (\mathbf{h}_{1,k} \mathbf{x}_r) + \operatorname{erf} (\mathbf{h}_{2,k} \mathbf{x}_r)}. \quad (49)$$

Note that $\frac{\partial g(\mathbf{x}_r)}{\partial \mathbf{x}_r}$ can be written in the form

$$\frac{\partial g(\mathbf{x}_r)}{\partial \mathbf{x}_r} = - \sum_{k=1}^K \frac{P_k(\mathbf{x}_r)}{Q_k(\mathbf{x}_r)} \quad (50)$$

where

$$P_k(\mathbf{x}_r) = \frac{2}{\sqrt{\pi}} e^{-(\mathbf{h}_{1,k}\mathbf{x}_r)^2} \mathbf{h}_{1,k} + \frac{2}{\sqrt{\pi}} e^{-(\mathbf{h}_{2,k}\mathbf{x}_r)^2} \mathbf{h}_{2,k} \quad (51)$$

$$Q_k(\mathbf{x}_r) = \text{erf}(\mathbf{h}_{1,k}\mathbf{x}_r) + \text{erf}(\mathbf{h}_{2,k}\mathbf{x}_r). \quad (52)$$

To compute the Hessian $\frac{\partial P_k(\mathbf{x}_r)}{\partial \mathbf{x}_r^T}$ and $\frac{\partial Q_k(\mathbf{x}_r)}{\partial \mathbf{x}_r^T}$ are calculated as

$$\frac{\partial P_k(\mathbf{x}_r)}{\partial \mathbf{x}_r^T} = -(\Psi_{1,k} + \Psi_{2,k}) \quad (53)$$

$$\frac{\partial Q_k(\mathbf{x}_r)}{\partial \mathbf{x}_r^T} = P_k(\mathbf{x}_r)^T, \quad (54)$$

where $\Psi_{1,k}$ and $\Psi_{2,k}$ read as

$$\Psi_{1,k} = \frac{4}{\sqrt{\pi}} e^{-(\mathbf{h}_{1,k}\mathbf{x}_r)^2} \mathbf{h}_{1,k}^T \mathbf{x}_r^T \mathbf{h}_{1,k}^T \mathbf{h}_{1,k} \quad (55)$$

$$\Psi_{2,k} = \frac{4}{\sqrt{\pi}} e^{-(\mathbf{h}_{2,k}\mathbf{x}_r)^2} \mathbf{h}_{2,k}^T \mathbf{x}_r^T \mathbf{h}_{2,k}^T \mathbf{h}_{2,k}. \quad (56)$$

The Hessian then reads as

$$\frac{\partial^2 g(\mathbf{x}_r)}{\partial \mathbf{x}_r \partial \mathbf{x}_r^T} = \sum_{k=1}^K \frac{P_k(\mathbf{x}_r)^T P_k(\mathbf{x}_r) + (\Psi_{1,k} + \Psi_{2,k}) Q_k(\mathbf{x}_r)}{Q_k(\mathbf{x}_r)^T Q_k(\mathbf{x}_r)}. \quad (57)$$

The Hessian is PSD if $(\Psi_{1,k} + \Psi_{2,k}) Q_k(\mathbf{x}_r) > 0 \forall k \in \{1, \dots, K\}$. Note that positive semi-definiteness is achieved for $\mathbf{h}_{1,k}\mathbf{x}_r \geq 0 \forall k \in \{1, \dots, K\}$ and $\mathbf{h}_{2,k}\mathbf{x}_r \geq 0 \forall k \in \{1, \dots, K\}$. Finally, the condition for convexity of the UBMSEP objective function can be cast as

$$\begin{bmatrix} \mathbf{H}_{R,\theta}^{s*} - \mathbf{H}_{I,\theta}^{s*} \\ \mathbf{H}_{R,\theta}^{s*} + \mathbf{H}_{I,\theta}^{s*} \end{bmatrix} \mathbf{x}_r \geq \mathbf{0}. \quad (58)$$

REFERENCES

- [1] L. U. Khan, I. Yaqoob, M. Imran, Z. Han, and C. S. Hong, "6G Wireless Systems: A Vision, Architectural Elements, and Future Directions," *IEEE Access*, vol. 8, pp. 147 029–147 044, 2020.
- [2] F. Rusek, D. Persson, B. K. Lau, E. G. Larsson, T. L. Marzetta, O. Edfors, and F. Tufvesson, "Scaling Up MIMO: Opportunities and Challenges with Very Large Arrays," *IEEE Signal Process. Mag.*, vol. 30, no. 1, 2013.
- [3] T. S. Rappaport, Y. Xing, O. Kanhere, S. Ju, A. Madanayake, S. Mandal, A. Alkhateeb, and G. C. Trichopoulos, "Wireless Communications and Applications Above 100 GHz: Opportunities and Challenges for 6G and Beyond," *IEEE Access*, vol. 7, pp. 78 729–78 757, 2019.

- [4] M. Giordani, M. Polese, M. Mezzavilla, S. Rangan, and M. Zorzi, "Toward 6G Networks: Use Cases and Technologies," *IEEE Commun. Mag.*, vol. 58, no. 3, pp. 55–61, 2020.
- [5] S. Elmeadawy and R. M. Shubair, "6G Wireless Communications: Future Technologies and Research Challenges," in *2019 Int. Conference on Electrical and Computing Technologies and Applications (ICECTA)*, Ras Al Khaimah, UAE, 2019.
- [6] P. Yang, Y. Xiao, M. Xiao, and S. Li, "6G Wireless Communications: Vision and Potential Techniques," *IEEE Netw.*, vol. 33, no. 4, pp. 70–75, 2019.
- [7] A. Mezghani and J. A. Nossek, "Power efficiency in communication systems from a circuit perspective," in *2011 IEEE International Symposium of Circuits and Systems (ISCAS)*, 2011, pp. 1896–1899.
- [8] —, "Modeling and minimization of transceiver power consumption in wireless networks," in *2011 International ITG Workshop on Smart Antennas*, 2011, pp. 1–8.
- [9] S. K. Mohammed and E. G. Larsson, "Per-Antenna Constant Envelope Precoding for Large Multi-User MIMO Systems," *IEEE Trans. Commun.*, vol. 61, no. 3, pp. 1059–1071, March 2013.
- [10] S. Jacobsson, G. Durisi, M. Coldrey, T. Goldstein, and C. Studer, "Quantized Precoding for Massive MU-MIMO," *IEEE Trans. Commun.*, vol. 65, no. 11, pp. 4670–4684, 2017.
- [11] A. Mezghani, D. Plabst, L. A. Swindlehurst, I. Fijalkow, and J. A. Nossek, "Sparse Linear Precoders For Mitigating Nonlinearities In Massive MIMO," in *2021 IEEE Statistical Signal Processing Workshop (SSP)*, 2021, pp. 391–395.
- [12] S. Jacobsson, G. Durisi, M. Coldrey, T. Goldstein, and C. Studer, "Nonlinear 1-bit precoding for massive MU-MIMO with higher-order modulation," in *2016 50th Asilomar Conference on Signals, Systems and Computers*, 2016, pp. 763–767.
- [13] S. Jacobsson, O. Castañeda, C. Jeon, G. Durisi, and C. Studer, "Nonlinear precoding for phase-quantized constant-envelope massive MU-MIMO-OFDM," in *2018 25th International Conference on Telecommunications (ICT)*, 2018.
- [14] A. Noll, H. Jedda, and J. Nossek, "PSK Precoding in Multi-User MISO Systems," in *WSA 2017; 21th International ITG Workshop on Smart Antennas*, Berlin, Germany, 2017, pp. 1–7.
- [15] A. Li, F. Liu, C. Masouros, Y. Li, and B. Vucetic, "Interference Exploitation 1-Bit Massive MIMO Precoding: A Partial Branch-and-Bound Solution With Near-Optimal Performance," *IEEE Trans. Wireless Commun.*, vol. 19, no. 5, pp. 3474–3489, 2020.
- [16] S. Jacobsson, W. Xu, G. Durisi, and C. Studer, "MSE-optimal 1-bit precoding for multiuser MIMO via branch and bound," in *Proc. IEEE Int. Conf. Acoust., Speech, Signal Process.*, Calgary, Alberta, Canada, April 2018, pp. 3589–3593.
- [17] E. S. P. Lopes and L. T. N. Landau, "Optimal and Suboptimal MMSE Precoding for Multiuser MIMO Systems Using Constant Envelope Signals with Phase Quantization at the Transmitter and PSK Modulation," in *WSA 2020; 24th International ITG Workshop on Smart Antennas*, Hamburg, Germany, 2020.
- [18] E. S. P. Lopes and L. T. N. Landau, "Discrete MMSE Precoding for Multiuser MIMO Systems with PSK Modulation," 2021.
- [19] P. V. Amadori and C. Masouros, "Constant envelope precoding by interference exploitation in phase shift keying-modulated multiuser transmission," *IEEE Trans. Commun.*, vol. 16, no. 1, pp. 538–550, Jan 2017.
- [20] H. Jedda, A. Mezghani, A. L. Swindlehurst, and J. A. Nossek, "Quantized constant envelope precoding with PSK and QAM signaling," *IEEE Trans. Wireless Commun.*, vol. 17, no. 12, pp. 8022–8034, Dec 2018.
- [21] F. Askerbeyli, W. Xu, and J. A. Nossek, "1-Bit Precoding for Massive MIMO Downlink with Linear Programming and a Greedy Algorithm Extension," in *2021 IEEE 93rd Vehicular Technology Conference (VTC2021-Spring)*, 2021, pp. 1–5.
- [22] G.-J. Park and S.-N. Hong, "Construction of 1-Bit Transmit-Signal Vectors for Downlink MU-MISO Systems With PSK Signaling," *IEEE Transactions on Vehicular Technology*, vol. 68, no. 8, pp. 8270–8274, 2019.
- [23] S. Hong, Y. Cho, and S. Park, "Construction of 1-Bit Transmit Signal Vectors for Downlink MU-MISO Systems: QAM constellations," *IEEE Transactions on Vehicular Technology*, pp. 1–1, 2021.

- [24] L. T. N. Landau and R. C. de Lamare, "Branch-and-bound precoding for multiuser MIMO systems with 1-bit quantization," *IEEE Wireless Commun. Lett.*, vol. 6, no. 6, pp. 770–773, Dec 2017.
- [25] E. S. P. Lopes and L. T. N. Landau, "Optimal Precoding for Multiuser MIMO Systems With Phase Quantization and PSK Modulation via Branch-and-Bound," *IEEE Wireless Commun. Lett.*, vol. 9, no. 9, pp. 1393–1397, 2020.
- [26] H. Jedda, J. A. Nossek, and A. Mezghani, "Minimum BER precoding in 1-bit massive MIMO systems," in *Proc. of IEEE Sensor Array and Multichannel Signal Processing Workshop (SAM)*, Rio de Janeiro, Brazil, July 2016.
- [27] M. Shao, Q. Li, W.-K. Ma, and A. M.-C. So, "A framework for one-bit and constant-envelope precoding over multiuser massive miso channels," *IEEE Transactions on Signal Processing*, vol. 67, no. 20, pp. 5309–5324, 2019.
- [28] F. Sahrabi, Y.-F. Liu, and W. Yu, "One-Bit Precoding and Constellation Range Design for Massive MIMO With QAM Signaling," *IEEE Journal of Selected Topics in Signal Processing*, vol. 12, no. 3, pp. 557–570, 2018.
- [29] M. Shao, Q. Li, and W.-K. Ma, "One-Bit Massive MIMO Precoding via a Minimum Symbol-Error Probability Design," in *2018 IEEE International Conference on Acoustics, Speech and Signal Processing (ICASSP)*, 2018, pp. 3579–3583.
- [30] M. Shao, Q. Li, W.-K. Ma, and A. M.-C. So, "Minimum Symbol Error Rate-Based Constant Envelope Precoding for Multiuser Massive MISO Downlink," in *2018 IEEE Statistical Signal Processing Workshop (SSP)*, 2018, pp. 727–731.
- [31] M. Shao, Q. Li, Y. Liu, and W.-K. Ma, "Multiuser One-Bit Massive MIMO Precoding Under MPSK Signaling," in *2018 IEEE Global Conference on Signal and Information Processing (GlobalSIP)*, 2018, pp. 833–837.
- [32] A. Mezghani and R. W. Heath, "Massive MIMO precoding and spectral shaping with low resolution DACs and active constellation extension," 2020.
- [33] B. Fesl, H. Jedda, and J. A. Nossek, "Discrete one-bit precoding for massive mimo," in *WSA 2019; 23rd International ITG Workshop on Smart Antennas*, April 2019, pp. 1–6.
- [34] G. Boole, *The Mathematical Analysis of Logic*. Philosophical Library, 1847.
- [35] S. Boyd and L. Vandenberghe, *Convex Optimization*. New York, NY, USA: Cambridge University Press, 2004.
- [36] S. Park, Y. Cho, and S. Hong, "Low-Complexity Symbol-Level Precoding for MU-MISO Downlink Systems with QAM Signals," 2021.
- [37] F. Sahrabi, Y.-F. Liu, and W. Yu, "One-Bit Precoding and Constellation Range Design for Massive MIMO With QAM Signaling," *IEEE Journal of Selected Topics in Signal Processing*, vol. 12, no. 3, pp. 557–570, 2018.
- [38] F. Askerbeyli, W. Xu, and J. A. Nossek, "1-Bit Precoding for Massive MIMO Downlink with Linear Programming and a Greedy Algorithm Extension," in *2021 IEEE 93rd Vehicular Technology Conference (VTC2021-Spring)*, 2021, pp. 1–5.
- [39] A. S. Belenky. Boston, MA: Springer US, 1998, pp. 91–124.
- [40] A. H. Land and A. G. Doig, "An Automatic Method of Solving Discrete Programming Problems," *Econometrica*, vol. 28, no. 3, pp. 497–520, 1960.
- [41] H. Yang and T. L. Marzetta, "Performance of conjugate and zero-forcing beamforming in large-scale antenna systems," *IEEE J. Sel. Areas Commun.*, vol. 31, no. 2, pp. 172–179, 2013.
- [42] O. Castañeda, S. Jacobsson, G. Durisi, T. Goldstein, and C. Studer, "VLSI Design of a 3-bit Constant-Modulus Precoder for Massive MU-MIMO," in *2018 IEEE International Symposium on Circuits and Systems (ISCAS)*, 2018, pp. 1–5.
- [43] M. Joham, W. Utschick, and J. A. Nossek, "Linear transmit processing in MIMO communications systems," *IEEE Trans. Signal Process.*, vol. 53, no. 8, pp. 2700–2712, Aug 2005.